Theoretical and numerical study of diffraction on electromagnetic optics VI. Obliquely incident t.e.-polarized gaussian beams on a finite grating with conducting substrate

O. Mata-Mendez and F. Chavez-Rivas
Departamento de Física, Escuela Superior de Física y Matemáticas, Instituto Politécnico Nacional, 07738 Zacatenco, México, D.F., México

J. Sumaya-Martinez
Facultad de Ciencias, Universidad Autónoma del Estado de México, Av. Instituto Literario No. 100, 50000 Toluca, Estado de México, México

Recibido el 4 de abril de 2003; aceptado el 16 de octubre de 2003

Diffraction of an obliquely incident TE-polarized Gaussian beams by N equally spaced slits (finite grating) with conducting substrate is treated. The substrate can be either vacuum or conductor. The diffracted and scattered patterns, the transmission and reflection coefficients, and the normally diffracted energy are analyzed as a function of several optogeometrical parameters. Particularly, the coupling between slits and the influence of the substrate is considered. We have found that, when the substrate is a conductor, the grating equation in reflection predicts with good precision the angular positions of the orders of a finite grating; the angular positions of these orders are independents of the beam width, the spot position on the finite grating, and the conductivity of the substrate. Besides, the envelope of the reflected energy is conserved constant when the position of the spot is changed.

Keywords: Diffraction; scattering; electromagnetic optics; gratings.

Se presenta una teoría rigurosa modal para la difracción de un haz Gausiano con polarización T.E. incidiendo oblicuamente sobre una red de difracción finita hecha de N rendijas. La pantalla donde están excavadas las rendijas es plana e infinitamente conductora, mientras que el sustrato puede ser un dieléctrico o un metal con índice de refracción complejo . Estudiamos el patrón de radiación en campo lejano, el coeficiente de transmisión y la energía normalmente difractada. Particularmente se analiza el acoplamiento entre rendijas y la influencia del sustrato.

Descriptores: Difracción; dispersión; óptica electromagnética; redes de difracción.

PACS: 42.25.Fx; 42.10.H.C

1. Introduction

The diffraction of beam waves has attracted a great deal of attention in recent years. Particularly, in visible and microwave regions where the diffraction by slits has been widely investigated because of their great amount of applications in the fields of acousto-optics, holography and spectroscopy [1]. However, the majority of the published papers consider only the diffraction of incident plane waves [2-14]. The diffraction of other types of waves such as the higher modes of emission of a laser [15], and particularly the fundamental TEM_{00}emission mode have been also studied.

In order to treat the general problem of the diffraction different approximate methods such as the scalar Rayleigh-Sommerfeld theory [16] and the Kirchhoff approach have been proposed. However, if accurate results are required, an electromagnetic rigorous theory of diffraction is necessary, especially within the so called vectorial region [16,17] defined by $\lambda/\ell \geq 0.2$, in opposition to the scalar region given by $\lambda/\ell < 0.2$, where λ is the wavelength and ℓ is the characteristic length of the apertures. As it is known, in the vectorial region of diffraction ($\lambda/\ell \geq 0.2$) the polarization effects become significant [16,17], so that, the scalar theories of diffraction can not be applied here.

In a previous paper [18] we treated the diffraction of a T.E. polarized normal incident Gaussian beam by one slit ruled onto a planar perfectly conducting screen with conducting substrate. In this paper we have extended the theory given in Ref. 18 to the case of an obliquely incident Gaussian beam on a finite grating made of N equally spaced slits with a substrate, which can be either vacuum or a conductor. The grating is ruled into a planar perfectly conducting thin screen. To our knowledge this case has not been studied rigorously in detail. In this paper the T.E polarization case (the incident electric field E_i is parallel to the slits) is considered, and in a future paper the T.M. mode (the incident magnetic field H_i is parallel to the slits) will be studied. We focus our attention to the vectorial region of diffraction, although the scalar region of diffraction is taken into account too.

It is important to mention that the problem which is treated in this paper is not only an interesting subject in the field of electromagnetic wave theory, but also it is an important one relating to the surface measurement or diagnostics by microwave, millimeter-wave, laser, or ultrasonic beams, and particularly to the development of various kinds of optical devices such as beam shapers, multiplexers, polarizers, spatial filters, and waveguide couplers [1].

2. Formulation of the theory

2.1. Angular plane wave expansion of the fields

N equally slits of width ℓ and separation d are ruled into a planar perfectly conducting thin screen, *i.e.*, we will consider a finite grating where the period is $D = \ell + d$ (see Fig. 1). We assume that the substrate can be either vacuum or a conductor. The position of a point in space is fixed by its Cartesian coordinates x, y, and z. Besides this, we consider an obliquely incident T.E.-polarized Gaussian beam, which is independent on the z-coordinate. The incident wave is a cylindrical wave. The harmonic time dependence of the complex field quantities is assumed to be of the form$\exp(-i\omega t)$. We notice that this model of a finite grating can be used also to consider a grating made (lamellar gratings) with conducting substrate. This lamellar grating can be simulated by taking the slit number N very large in our finite grating.

From the uniqueness of the solution and the invariance of the field along the $z-$coordinate, we get that the total field E depends only on the coordinates x and y. Then, our original vector problem becomes a scalar one with an unknown function $E(x, y)$ given by the component of the electric field along the Oz-axis which satisfies the two-dimensional version of the Helmholtz equation

$$\frac{\partial^2 E}{\partial x^2} + \frac{\partial^2 E}{\partial y^2} + k^2 E = 0, \tag{1}$$

where $k = k_0 n$, $k_0 = 2\pi/\lambda$ is the module of the wave vector in vacuum, and n is the refractive index of the medium, which is a complex number for the substrate. This equation is a second order partial differential equation which we need to treat in order to solve the problem posed in this paper.

It is convenient to take the Fourier transform of the field $E(x, y)$ along the Ox-axis as

$$E(x, y) = \frac{1}{\sqrt{2\pi}} \int_{-\infty}^{\infty} \hat{E}(\alpha, y) \exp(i\alpha x) d\alpha, \tag{2}$$

where the inverse Fourier transform $\hat{E}(\alpha, y)$is given by

$$\hat{E}(\alpha, y) = \frac{1}{\sqrt{2\pi}} \int_{-\infty}^{\infty} E(x, y) \exp(-i\alpha x) d\alpha. \tag{3}$$

Observe that the spectral amplitude $\hat{E}(\alpha, y)$ of the electric field $E(x, y)$ can be directly handle with the last transformation.

After substituting Eq.(2) into Eq. (1) we get an ordinary second order differential equation in $\hat{E}(\alpha, y)$ which solution is immediately obtained. For this, it is necessary to distinguish among the upper-region $(y > 0)$ and the lower-region$(y < 0)$ of our configuration

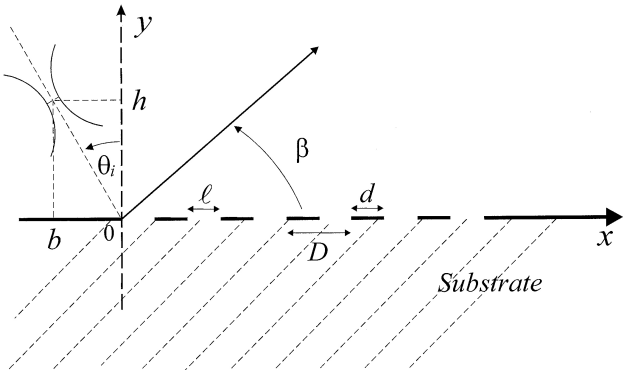

FIGURE 1. Our configuration composed of N slits of width ℓ and separation d, *i.e.* of period $D = \ell + d$ in a planar perfectly conducting screen with conducting substrate. The slits are parallel to the *Oz* axis. We assume an obliquely incident Gaussian beam at the angle θ_i.

$$\hat{E}_1(\alpha, y) = A(\alpha) \exp(-i\beta y) + B(\alpha) \exp(i\beta y) \quad (\text{for } y > 0), \tag{4}$$

$$\hat{E}_2(\alpha, y) = C(\alpha) \exp(-i\beta_c y) + D(\alpha) \exp(i\beta_c y) \quad (\text{for } y < 0), \tag{5}$$

where we have the following definitions $\beta^2 = k_0^2 - \alpha^2$ with $\text{Im}(\beta) \geq 0$, and $\beta_c^2 = k^2 - \alpha^2$ with $\text{Im}(\beta_c) \geq 0$. The wave vector k is a complex number, because in general the substrate is a conductor.

Before to continue with the solution of our problem it is convenient to analyze Eqs. (4) and (5). The first term of Eq. (4) is related with the Fourier transform of the incident beam E_i (incoming wave), with amplitude $A(\alpha)$. This function $A(\alpha)$ is very important in order to consider the shape of the incident spot, in fact, with this function we can simulate a Gaussian beam, a Hermite-Gaussian beam, and so on. In this paper we concentrate our attention to the Gaussian beam, but in a following paper the case of Hermite-Gaussian beams will be discussed. The second term given by $B(\alpha)$ represents the scattered wave. This field is composed of an infinite number of plane waves dispersed by the slits, some of them are propagating outgoing waves $(|\alpha| < k_0)$, while others are evanescent waves $(|\alpha| > k_0)$. These evanescent fields are necessary in order to coupling the upper-region and the bottom-region and their behavior are similar to that of the problem of the well potential encountered in quantum mechanics. Finally, the total field below the screen given by Eq.(5) which is composed of the coefficients $C(\alpha)$ and $D(\alpha)$. Besides, $A(\alpha) = 0$ for $|\alpha| > k_0$ and $D(\alpha) = 0$ for all α, since the field should be bounded for $y \to \pm\infty$. Observe that this solution satisfies the required outgoing wave condition or Sommerfeld's radiation condition. In conclusion, it follows from Eqs.(2) to (5) that the electric fields E_1 and E_2 can be expressed by an infinite

number of plane waves and evanescent waves as follow:

$$E_1(x,y) = \frac{1}{\sqrt{2\pi}} \int_{-k_0}^{k_0} A(\alpha) e^{i(\alpha\, x - \beta\, y)} d\alpha + \frac{1}{\sqrt{2\pi}} \int_{-\infty}^{\infty} B(\alpha) e^{i(\alpha\, x + \beta\, y)} d\alpha \ (\text{for } y > 0), \quad (6)$$

$$E_2(x,y) = \frac{1}{\sqrt{2\pi}} \int_{-\infty}^{\infty} C(\alpha) e^{i(\alpha\, x - \beta_c\, y)} d\alpha \ (\text{for } y < 0), \quad (7)$$

these expressions correspond to the so called angular plane-wave expansions. We notice that the + sign at the exponentials means that we have up propagating waves, while the - sign means down propagating waves.

Let $E_3(x, y = 0)$ be the electric field at $y = 0$, which have be null at the screen in the model of infinite conductivity considered here. It is convenient to mention that this model is valid for microwave and radio wave regions, therefore, for the diffraction in the visible region it is necessary to consider the finite conductivity of the screen. From this, it follows that E_3 can be expressed as

$$E_3(x,0) = \sum_{n=1}^{\infty} a_{n1}\phi_{n1}(x) + \sum_{n=1}^{\infty} a_{n2}\phi_{n2}(x) + \ldots + \sum_{n=1}^{\infty} a_{nN}\phi_{nN}(x), \quad (8)$$

where the functions $\phi_{np}(x)$ (with $p = 1, 2, \ldots, N$) are given by

$$\phi_{np} = \begin{cases} \sin\left[(x - (p-1)\,(d+\ell))\,\frac{n\pi}{\ell}\right] & \text{if} \quad (p-1)\,(d+\ell) \le x \le \ell + (p-1)\,(d+\ell) \\ 0 \text{ elsewhere } x \end{cases}, \quad (9)$$

the coefficients a_{np} are the so called modal coefficients. The functions $\phi_{np}(x)$ constitute a basis with the following orthogonality condition

$$\langle \phi_{np}, \phi_{mq} \rangle = \int_{-\infty}^{\infty} \phi_{np}\phi^*_{mq} dx = \frac{\ell}{2}\delta_{nm}\delta_{pq}, \quad (10)$$

with $n, m = 1, 2, \ldots \infty$ and $p, q = 1, 2, \ldots, N$. From Eq.(9) we see that functions $\phi_{np}(x)$ are sine functions over the slits and null along the screen.

From Eqs. (6), (7), and (8) we have the expressions of the total electric field at the upper-region, at the lower-region, and on the screen. To finish completely our diffraction problem it is necessary to determine the functions $B(\alpha), C(\alpha)$, and the set of modal coefficients $a_{n1}, a_{n2}, \ldots, a_{nN}$. For this, we have to use the boundary conditions given by the continuity of the tangential component and the normal derivative of the electric field at $y = 0$. It is important to notice that this two-dimensional problem requires only two boundary conditions.

2.2. Conditions of continuity

From the continuity of the electric fields E_1 and E_3, and, of the fields E_2 and E_3 at $y = 0$, we obtain from Eqs. (4), (5), and (8) the following equations

$$A(\alpha) + B(\alpha) = \sum_{n=1}^{\infty} a_{n1}\hat{\phi}_{n1}(\alpha) + \sum_{n=1}^{\infty} a_{n2}\hat{\phi}_{n2}(\alpha) + \ldots + \sum_{n=1}^{\infty} a_{nN}\hat{\phi}_{nN}(\alpha) \quad (11)$$

$$C(\alpha) = \sum_{n=1}^{\infty} a_{n1}\hat{\phi}_{n1}(\alpha) + \sum_{n=1}^{\infty} a_{n2}\hat{\phi}_{n2}(\alpha) + \ldots + \sum_{n=1}^{\infty} a_{nN}\hat{\phi}_{nN}(\alpha), \quad (12)$$

where $\hat{\phi}_{np}(\alpha)$ is the Fourier transform of $\phi_{np}(x)$ with $n = 1, 2, \ldots, \infty$ and $p = 1, 2, \ldots, N$

In addition, the continuity of the normal derivative of E at $y = 0$, and x within the slits, and the fact that $\phi_{mq}(x)$ is null on the screen give us the following relationship:

$$\left\langle \frac{\partial\, E_1}{\partial\, y}(x,0) - \frac{\partial\, E_2}{\partial\, y}(x,0), \phi_{mq}(x) \right\rangle = 0. \quad (13)$$

By applying the Parseval-Plancherel theorem

$$\langle f(x), g(x) \rangle = \left\langle \hat{f}(\alpha), \hat{g}(\alpha) \right\rangle,$$

to Eq. (13), we get

$$\left\langle \frac{\partial\, \hat{E}_1}{\partial\, y}(\alpha,0) - \frac{\partial\, \hat{E}_2}{\partial\, y}(\alpha,0), \hat{\phi}_{mq}(\alpha) \right\rangle = 0, \quad (14)$$

with $m = 1, 2, \ldots, \infty$ y $q = 1, 2, \ldots, N$

Finally, if we obtain the derivative of Eqs.(4) and (5), and substituting them into Eq.(14), the unknowns $B(\alpha)$ and $C(\alpha)$ can be eliminated by using Eqs. (11) and (12). After these calculations the following equations are obtained for the un-

knowns modal coefficients a_{np}:

$$\sum_{n=1}^{\infty} a_{n1} \left\langle (\beta+\beta_c)\hat{\phi}_{n1}, \hat{\phi}_{mq} \right\rangle + \sum_{n=1}^{\infty} a_{n2} \left\langle (\beta+\beta_c)\hat{\phi}_{n2}, \hat{\phi}_{mq} \right\rangle + \ldots + \sum_{n=1}^{\infty} a_{nN} \left\langle (\beta+\beta_c)\hat{\phi}_{nN}, \hat{\phi}_{mq} \right\rangle = 2 \left\langle \beta A(\alpha), \hat{\phi}_{mq} \right\rangle, \quad (15)$$

with $m = 1, 2, \ldots, \infty$, and $q = 1, 2, \ldots, N$.

With these computations we have been able to reduce the problem of the diffraction of a beam wave by a finite grating made of N slits to a linear algebraic system with unknowns given by the modal coefficients. We have to mention, that this is not the only possible method of solution, since problems within the vectorial region are frequently solved by means of Fredholm type integral equations. It is important to note that the diffraction patterns are accurately determined from these modals coefficients, in fact, all the quantities of interest can be expressed in terms of these constants, thus, simplifying the numerical computations.

The conservation of energy is satisfied with these values of no within a precision of better than 10^{-4}. The modal coefficients a_{np} have been obtained numerically from Eq. (15) by using the Gauss-Seidel algorithm. From the modal coefficients and Eq. (8) the electric field inside the slits can be calculated. After substituting these modal coefficients a_{np}. into Eqs. (11) and (12) the spectral amplitudes $B(\alpha)$ and $C(\alpha)$ are also obtained. By inserting these expressions into Eqs. (6) and (7) the scattered and diffracted fields are finally calculated. Thus, the solution of the diffraction problem is formally and numerically given.

2.3. The theorem of conservation of energy

In order to establish the theorem of conservation of energy it is important to define the way the diffracted and scattered energies are calculated. Due to the fact that above the finite grating we have vacuum, let R be the reflection coefficient given by the ratio between the scattered energy and the incident energy I_0. From the complex Pointing vector R takes the following form

$$R = \frac{\int_{-k_0}^{k_0} \beta(\alpha) \left|B(\alpha)\right|^2 d\alpha}{\int_{-k_0}^{k_0} \beta(\alpha) \left|A(\alpha)\right|^2 d\alpha}. \quad (16)$$

For the transmitted energy it is necessary to distinguish between the cases when the substrate is either vacuum or conductor. In the first case, let T be the transmission coefficient defined as the ratio between the transmitted energy through the N slits and the incident energy I_0 which is given by

$$T = \frac{\int_{-k_0}^{k_0} \beta(\alpha) \left|C(\alpha)\right|^2 d\alpha}{\int_{-k_0}^{k_0} \beta(\alpha) \left|A(\alpha)\right|^2 d\alpha}, \quad (17)$$

from which the theorem of conservation of energy is written as follows:

$$R + T = 1. \quad (18)$$

However, in the case where the substrate is conductor, the refractive index is complex, we will talk now of the A energy absorbed by the substrate normalized to the incident energy, thus, the conservation of the energy is given by

$$R + A = 1, \quad (19)$$

where R is given by Eq.(16).

2.4. The obliquely incident Gaussian beam

As an incident electromagnetic wave, the two-dimensional version of a Gaussian beam will be considered. On the screen, and at normal incidence this field is given by [17]

$$E(x, y = 0) = \exp\left[-\frac{2\,(x-b)^2}{L^2}\right]. \quad (20)$$

From this expression the beam spectral amplitude for an obliquely incident Gaussian beam can be obtained

$$A(\alpha) = \frac{L}{2}(\cos\theta_i + \frac{\alpha}{\beta} sen\theta_i) \times \exp\left[i(-\alpha b + \beta h)\right] \exp(-\gamma^2/2), \quad (21)$$

where θ_i is the angle of incidence with respect to the Oy-axis. The position of the waist of the incident beam is given by b (the alignment with respect to the *Oy*-axis) and h, with h=0 from now on, (see Fig. 1). We denote by L the local $(1/e)$-intensity Gaussian beam diameter (L-spot diameter) which is a basic beam parameter, and $\gamma = (\alpha\cos\theta_i - \beta\,\mathrm{sen}\,\theta_i)L/2$. Where the intensity is defined by $I = cE^2$, with c a constant.

Unless otherwise is stated, throughout the paper the beam position will be kept fixed at $b = \Lambda\,/\,2$, where Λ is the total length of the system composed by N slits and N-1 separations d, *i.e.* the beam will be focused at the center of the finite grating. In addition, we call attention to the fact that the present theory is valid not only for Gaussian beams, but also for Hermite-Gaussian beams [19,20].

In order to assure accuracy of the numerical results, in all the simulations the energy-balance criterion has been always satisfied within a precision of better than 10^{-4}, which is the precision usually accepted in the literature. Before we continue, we would like to point out that the numerical results reported below are illustrated for some particular wavelengths λ/ℓ; nevertheless conclusions will also be valid for any value within the vectorial region, where $\lambda/\ell > 0.2$.

3. Numerical results: angular transmitted energy

In Ref. 21 the case of the diffraction of a normally incident TE polarized Gaussian beam by a finite grating was treated, where the substrate is vacuum. In this section we consider the same configuration but with an obliquely incident Gaussian beam where the substrate is vacuum. It is interesting to compare among the results obtained here at oblique incidence with those at normal incidence from Ref. 21. This comparison shows us with surprise that the case at normal incidence is very different to the case at oblique incidence. In all the results the slit width will be taken as ℓ=1 and the angle of incidence as $\theta_i = 30°$.

As we have seen, it is possible to consider the reflected energy and the transmitted energy by the grating, but in order to compare our results with those of Ref. 21 we only analyze the energy transmitted. However, in the next section the reflected energy will be taken into account.

3.1. Influence of the wavelength

First, the evolution of the far-field radiation pattern when the wavelength increases is considered. Figures 2 (semilog plots) show the diffraction from ten slits of normalized period $D/\ell = 2.0$, illuminated by an obliquely incident Gaussian beam **($\theta_i = 30°$)** of width $L/\ell = 20/\sqrt{2}$, with wavelengths $\lambda/\ell = 0.1$, 0.8, 1.5 and 2.5. The diffraction patterns of Fig. 2a shows the typical sharp orders resembling those of the diffraction of plane waves by a grating. However, as the ratio λ/ℓ comes into the vectorial zone, the number of oscillations decreases and the orders become wider. The maximum energy transmitted occurs at $\theta = 60°$ (see Fig.1) for any considered wavelength. Notice that the symmetry presented in Fig. 3 of Ref. 21 at normal incidence is broken here. Furthermore, we have found that the order positions agree very well with the predictions given by the classical grating rule.

In Fig. 3a we have plotted the energy diffracted normally E as a function of the wavelength for the diffraction of an obliquely incident Gaussian beam ($\theta_i = 30°$**)** of width $L/\ell = 5/\sqrt{2}$ by 2, 4, and 8 slits of period $D/\ell = 1.5$; unless otherwise indicated, this period will be used in what follows. It is surprising to verify that these results are very different to those obtained at normal incidence in Fig.4 of Ref. 21. In Fig.3b we have the transmission coefficient T as a function of the wavelength. It is interesting to see that the maxima in Fig.4a have the same positions that the maxima from Fig.4b, a similar conclusion can be obtained from Fig.4(a) of Ref. 21.

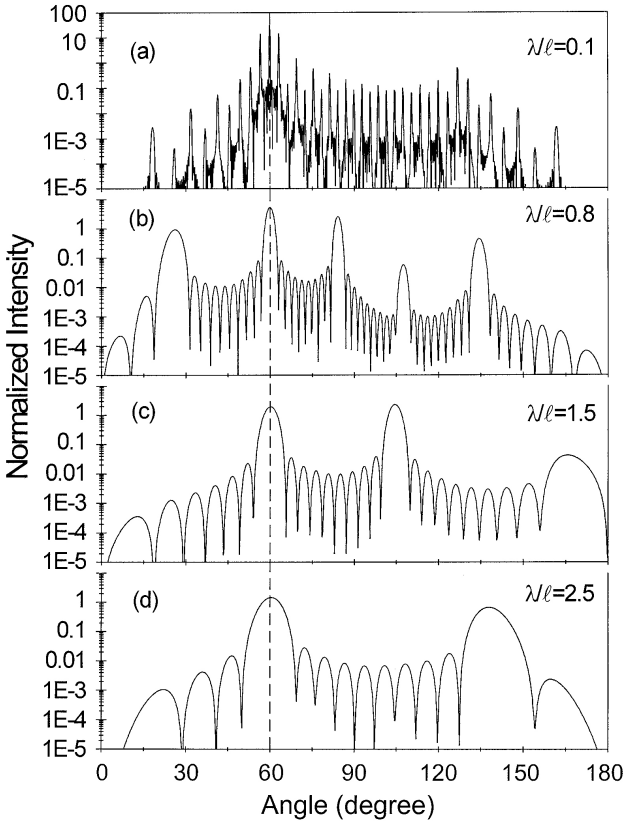

FIGURE 2. Logarithm of the diffracted intensity normalized to the total incident energy $\log(I(\theta)/I_0)$ for 10 slits of period $D/\ell = 2.0$. With $\theta_i = 30^0$, $L/\ell = 20/\sqrt{2}$, $b/\ell = 9.5$, and wavelengths: (a) $\lambda/\ell = 0.1$, (b) $\lambda/\ell = 0.8$, (c) $\lambda/\ell = 1.5$, and (d) $\lambda/\ell = 2.5$.

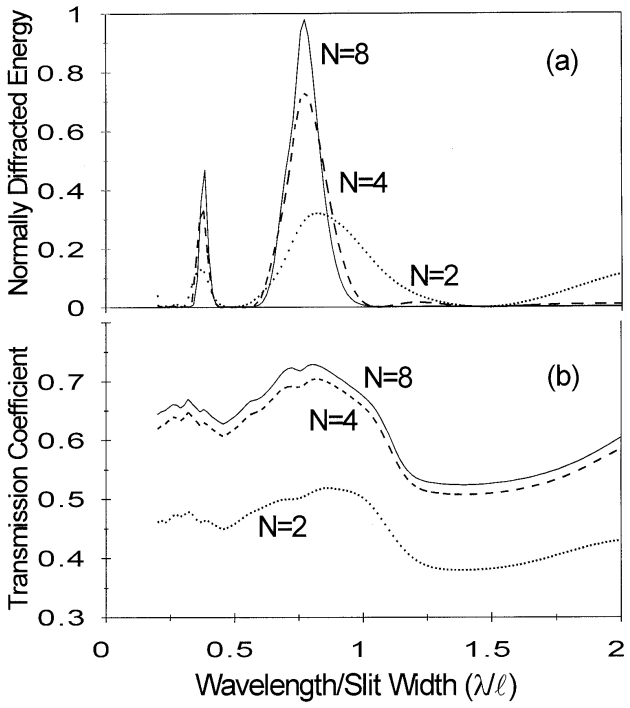

FIGURE 3. (a) Intensity diffracted at normal direction normalized to the total incident energy, and (b) transmission coefficient as a function of the normalized wavelength for a finite grating composed of 2, 4, and 8 slits of period $D/\ell = 1.5$. With $L/\ell = 5/\sqrt{2}$ and $\theta_i = 30°$, the beam waist is located at the middle of the finite grating.

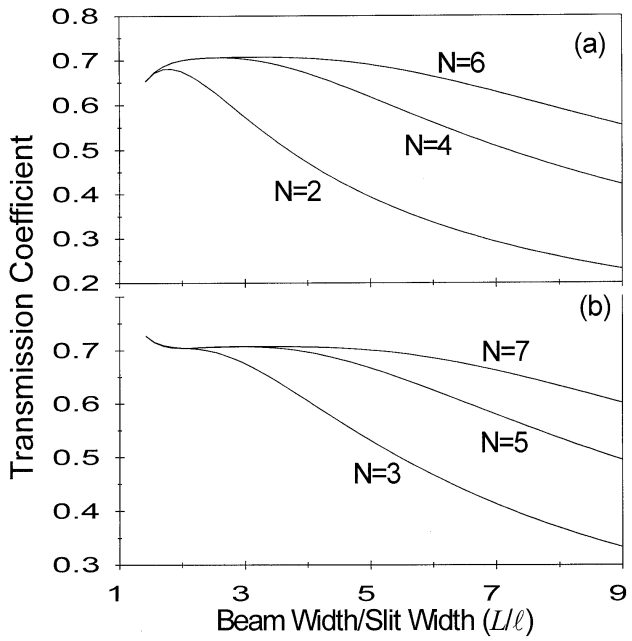

FIGURE 4. Transmission coefficient as a function of the normalized beam width (L/ℓ) for a finite grating of (a) 2,4,6 slits, and (b) 3,5,7 slits of period $D/\ell = 1.5$ with wavelength $\lambda/\ell = 0.9$. The beam waist is located at the middle of the finite grating.

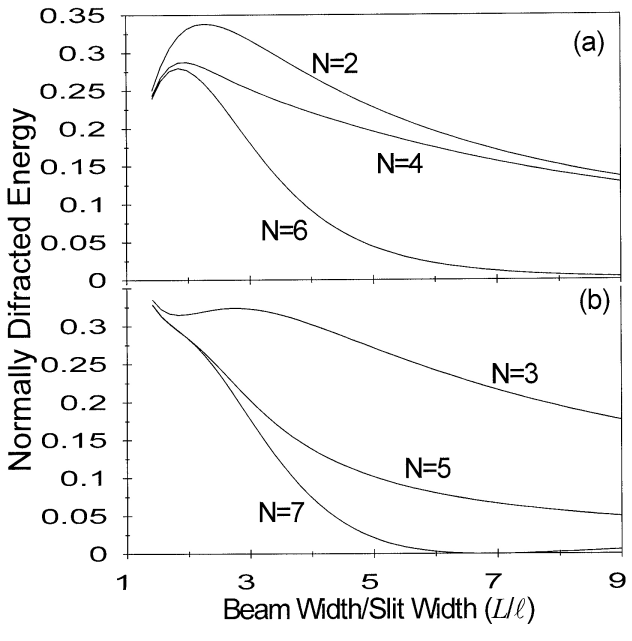

FIGURE 5. Intensity diffracted at normal direction normalized to the total incident energy (E/I_0) as a function of the normalized beam width (L/ℓ). Parameters are set as in Fig. 4.

3.2. Influence of the beam width

In Figs. 4 and 5 the transmission coefficient and the normalized diffracted energy are plotted as a function of the beam width L/ℓ. An obliquely incident Gaussian beam ($\theta_i = 30°$**)** of wavelength $\lambda/\ell = 0.9$ is assumed. In these cases the results are very similar to those shown in Ref. 21 at normal incidence, except in Fig. 5b where a very important discrepancy is present.

The evolution of the diffraction patterns when the beam width increases is depicted in Fig. 6, for an obliquely incident Gaussian beam at $\theta_i = 30°$**,** with a wavelength of $\lambda/\ell = 0.9$, and a finite grating made of 15 slits. Firstly, Fig. 6a shows the far-field pattern for a narrow incident beam of width $L/\ell = 7/\sqrt{2}$ (note that the beam waist covers not even half of the finite grating). Wide orders can be observed and, instead of secondary maxima, broad and very deep minima occur. In Fig. 6b a beam of width $L/\ell = 10/\sqrt{2}$ covers almost half of the finite grating making secondary maxima be visible. In Fig. 6c the finite grating is completely covered by a spot of width $L/\ell = 50/\sqrt{2}$. Finally, in Fig. 6d a very wide incident beam of $L/\ell = 500/\sqrt{2}$ (resembling a plane wave) makes the half-width of primary and secondary maxima become more narrow. It is remarkable to note that the angular position of the orders remains fixed, no matter what the beam width is given. On comparing Fig.6 with the corresponding Fig. 7 of Ref. 21 at normal incidence, we can see that the zero order is located at $\theta = 60°$ (30° measured from the normal) and the symmetry of these figures is lost.

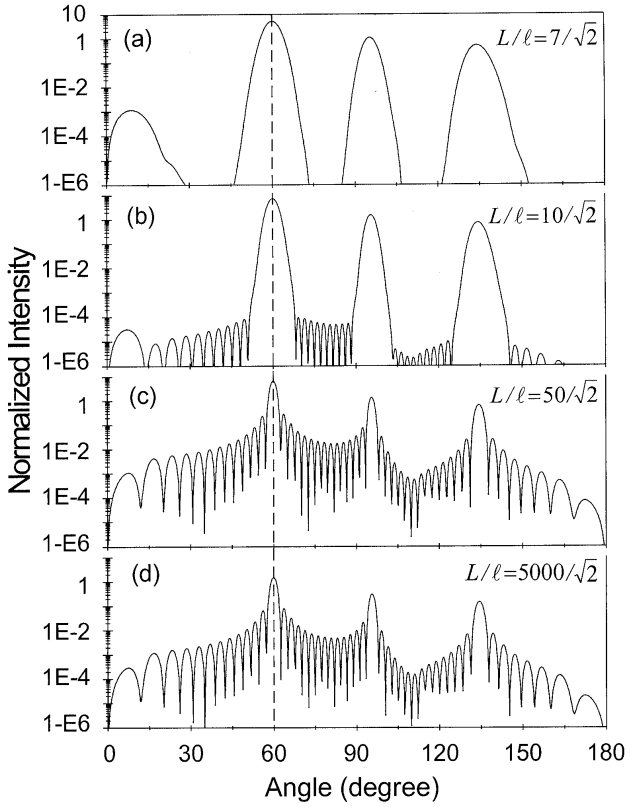

FIGURE 6. Logarithm of the normalized diffracted intensity $\log(I(\theta)/I_0)$ for a finite grating with 15 slits of period $D/\ell = 1.5$. With $\theta_i = 30°$,wavelength $\lambda/\ell = 0.9$, beam position $b/\ell = 11.0$, and beam widths (a) $L/\ell = 7/\sqrt{2}$, (b) $L/\ell = 10/\sqrt{2}$, (c) $L/\ell = 50/\sqrt{2}$, and (d) $L/\ell = 5000/\sqrt{2}$.

3.3. Influence of the beam position

Figure 7 shows the normally diffracted energy and the transmission coefficient as a function of the beam position for a finite grating made of 5 slits. For an obliquely incident ($\theta_i = 30°$) Gaussian beam, with $\lambda/\ell = 0.9$, and beam width $L/\ell = 50/\sqrt{2}$. In Ref. 21 we have shown that the corresponding results are described by a Gaussian function. However, from the results of Fig. 7 we see that for oblique incidence we have no Gaussian function, in fact for the normally diffracted energy we have found a minimum instead of the maximum usually encountered at normal incidence.

3.4. Coupling between slits

The transmission coefficient as a function of the separation d/ℓ between slits for the particular case of two slits was already studied in Ref. 22 for a TE-polarized normally incident Gaussian beam, and in Ref. 23 for a TM-polarized normally incident Gaussian beam, and the following results were obtained: (1) coupling produces an oscillate-decreasing behavior as the separation between slits increases, and (2) the period for these oscillations is exactly λ. We have obtained the same conclusion for a T.E.-polarized normally incident Gaussian beam on a finite grating as shown in Fig. 9 of Ref. 21.

Figure 8 shows the transmission coefficient as a function of the separation d/ℓ for a finite grating made of 3 and 5 slits. An obliquely incident Gaussian beam ($\theta_i = 30°$**)** of wavelength $\lambda/\ell = 0.9$ was used. To uniformly illuminate every each slit the beam width has been taken as $L/\ell = 500/\sqrt{2}$. From Fig.8 we observe with surprise that the conclusions obtained at normal incidence are no longer valid at oblique incidence. We see an oscillating behavior but in this case the period of oscillation is 2λ in place of λ (occurring at normal incidence). This result motive us to analyze in detail other cases, but this will be done in a future publication.

3.5. Non-periodic finite grating

Finally, we consider two finite gratings with $N = 6$, $d/\ell = 0.5$, and $D/\ell = 1.5$, joined with a different metal separation $d/\ell = 0.1$, 0.45, and 5.0. In Fig. 9 we show the diffraction patterns obtained with an obliquely incident Gaussian beam at $\theta_i = 30°$, with width $L/\ell = 20/\sqrt{2}$, and $\lambda/\ell = 0.9$. The spot is located at the middle of the finite non-periodic grating.

We note that the diffraction patterns resemble more a rough surface than the corresponding spectra of a finite grating. It is interesting to note that the highest maximum is located at $\theta = 60°$, where must be located the order zero of a grating. The results of Fig.9 have drastically changed with respect to those given in Fig. 10 of Ref. 21.

4. Numerical results: angular reflected energy

In Sec. 3 we have analyzed the angular transmitted energy when the substrate is vacuum, and in this section we consider the angular reflected energy when the substrate is either vacuum or a conductor. The complex refractive index of the sub-

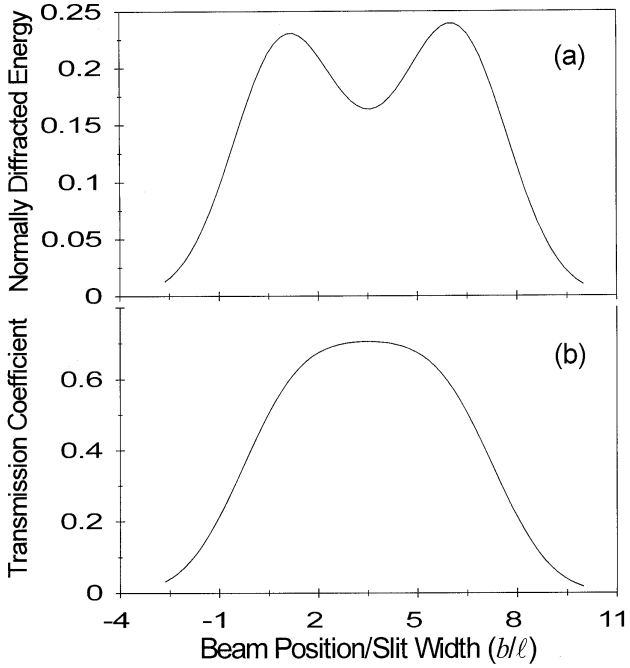

FIGURE 7. (a) Intensity diffracted at normal direction normalized to the total incident energy (E/I_0), and (b) transmission coefficient τ versus the normalized beam position (b/ℓ) for a finite grating of 5 slits of period $D/\ell = 1.5$. With $\lambda/\ell = 0.9$ and $L/\ell = 50/\sqrt{2}$.

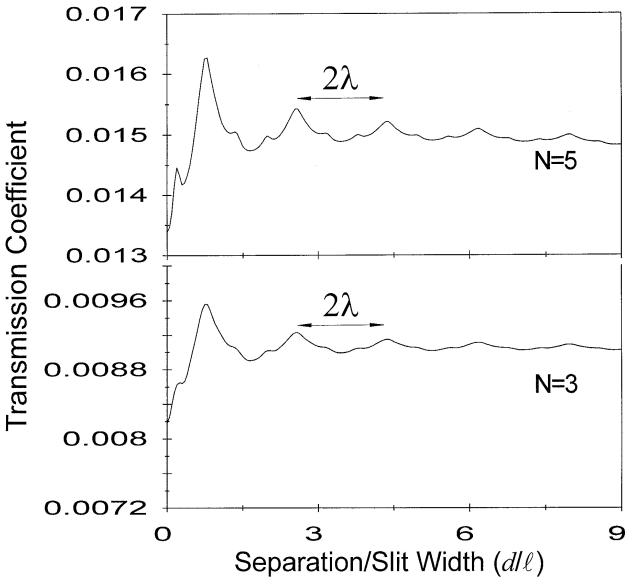

FIGURE 8. Coupling between slits. Transmission coefficient as a function of the normalized separation (d/ℓ) for a finite grating with $N = 3$ and $N = 5$ slits of period $D/\ell = 1.5$. With $\lambda/\ell = 0.9$, $L/\ell = 500/\sqrt{2}$, and $b/\ell = 0.5$.

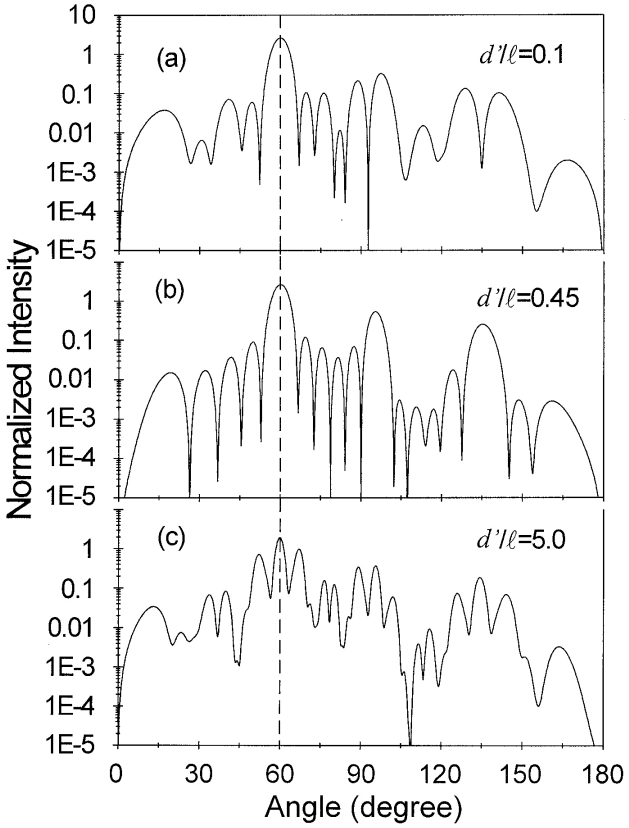

FIGURE 9. Diffracted intensity normalized to the total incident energy $(I(\theta)/I_0)$ for a finite nonperiodic grating with 6 slits of original period $D/\ell = 1.5$ and metal separation $d/\ell = 0.5$ where the mid-separation has been replaced by $d'/\ell = 0.1,\ 0.45,$ and 5.0. For $L/\ell = 20/\sqrt{2}$, $\lambda/\ell = 0.9$. The beam waist is placed at the middle of the finite non-periodic gratings.

strate n has been obtained by interpolation from *Handbook of optical constants of solids* by Edward D. Palik [24].

4.1. Influence of the beam position

In all the cases considered in this Sec.4.1 we plotted the angular scattered energy for a finite grating made of 10 slits with width slit $\ell = 1\mu$m and period $D = 2\mu$m. We also have an obliquely incident Gaussian beam with $\theta_i = 30°$, wavelength $\lambda = 0.8\mu$m, and width spot $L = 20/\sqrt{2}\mu$m.

In Fig. 10 we have plotted the angular scattered energy when the substrate is vacuum. In Fig. 10a the spot is centered at the finite grating, ($b/\ell = 9.5$, see Fig. 1), and in Fig.10b the centre of the spot is located at the edge of the finite grating ($b/\ell = 0$, see Fig. 1). These two figures show us the influence of the beam position in the angular distribution of the energy. In both of them, we notice the presence of five orders predicted by the grating equation for reflection given by $\cos\beta_n = \sin\theta_i + n\lambda/D$, see Fig.1. The maximum relative error between the positions of the orders given by our calculation and those from the grating equation is 1.3%.

From the results of Figs.10a and 10b two important general facts can be obtained:

1) We can say that for an incident Gaussian beam the grating equation in reflection predicts the angular positions of the orders of a finite grating with good precision, *i.e.*,

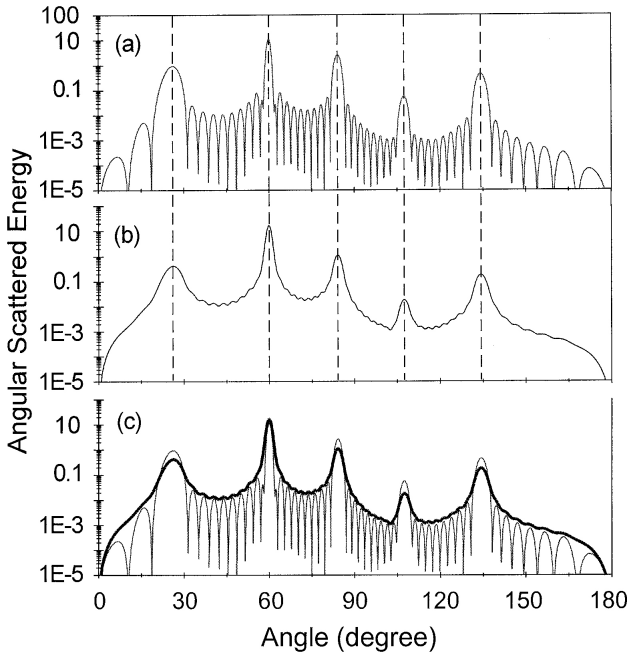

FIGURE 10. Angular scattered energy when the substrate is vacuum. For a finite grating made with 10 slits with width slit $\ell = 1\mu$m and period $D = 2\mu$m. The angle of incidence is $\theta_i = 30°$, the wavelength $\lambda = 0.8\mu$m, and the width spot $L = 20/\sqrt{2}\mu$m. In (a) the spot is centered at the finite grating ($b/\ell = 9.5$), in (b) the centre of the spot is located at the edge of the finite grating ($b/\ell = 0$), and in (c) we have superimposed (a) and (b).

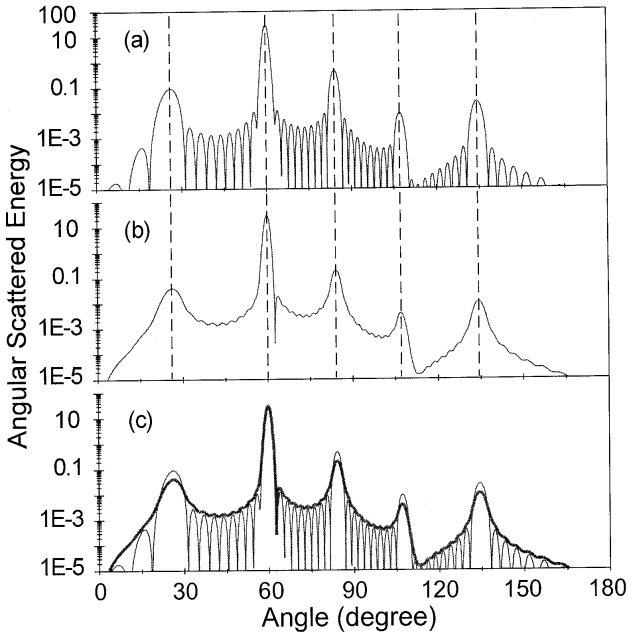

FIGURE 11. Same parameters as in Fig.10 but the substrate is lithium.

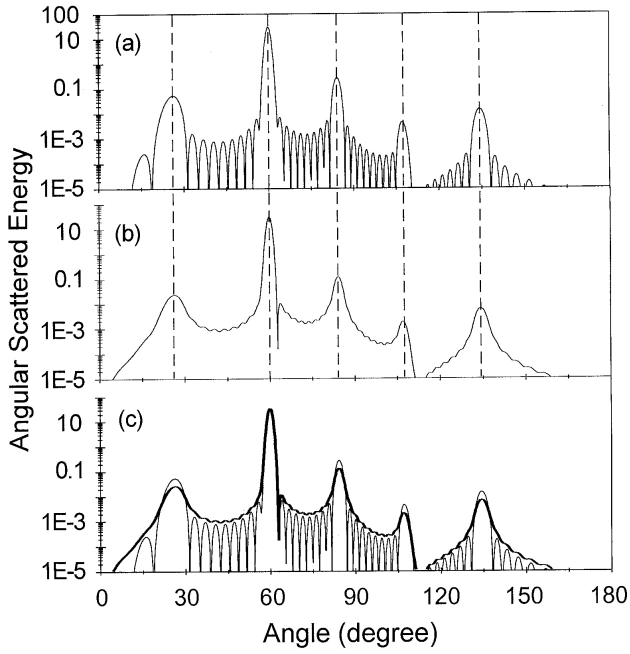

FIGURE 12. Same parameters as in Fig. 10 but the substrate is gold.

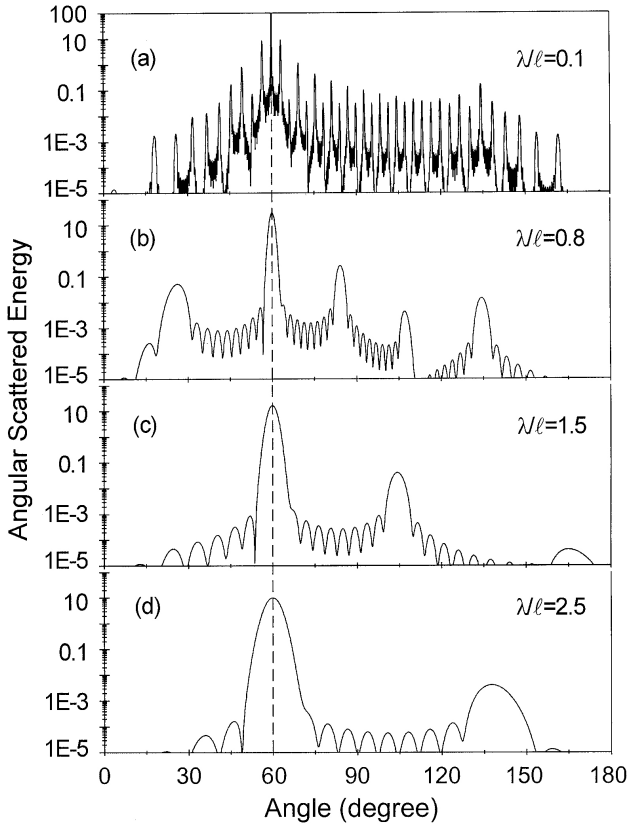

FIGURE 13. Influence of the wavelength on the angular reflected energy when the substrate is gold. For a finite grating with N=10 slits and period $D/\ell = 2.0$, when is illuminated by an obliquely incident Gaussian beam ($\theta_i = 30^0$) of width $L/\ell = 20/\sqrt{2}$, for the wavelengths λ/ℓ =0.1, 0.8, 1.5, and 2.5.

the angular positions of these orders are independents of the beam width and the position of the spot on the finite grating.

2) In Fig. 10c we have superimposed the Figs. 10a and 10b. We get from Fig. 10c that the envelope of the reflected energy is conserved constant when the position of the spot is changed along the finite grating (except for the reflected orders).

3) The last conclusions are also true for a conductor substrate. Besides, the angular positions of these orders are independents of the conductivity. These facts are shown in Figs.11 and 12 with the same parameters as in Fig. 10 but the substrate is lithium in Fig.11 and gold in Fig. 12. Also, these plots show how the scattered energy changes when the conductivity of the substrate is increased.

4.2. Influence of the wavelength

In Fig. 13 we show the influence of the wavelength on the angular reflected energy when the substrate is gold. We consider a finite grating made of 10 slits of normalized period $D/\ell = 2.0$, illuminated by an obliquely incident Gaus-

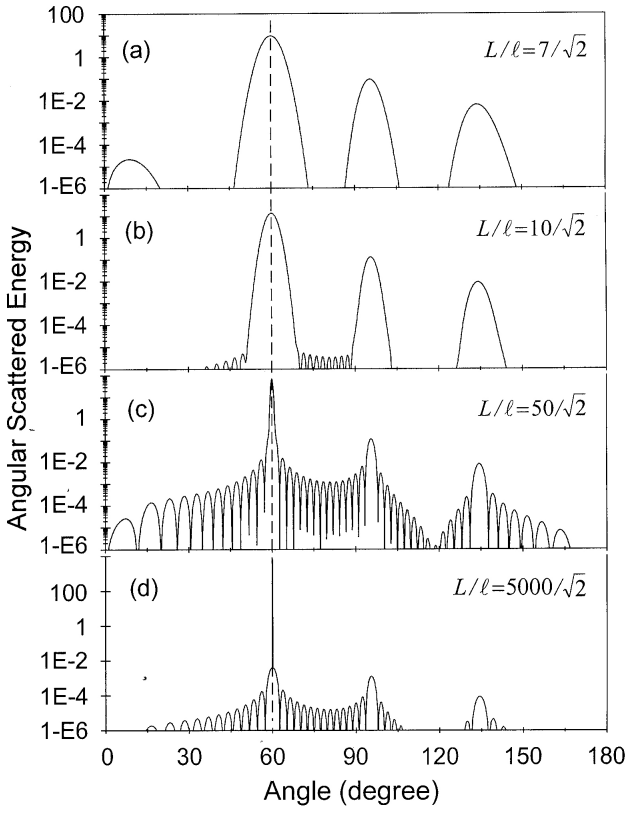

FIGURE 14. Influence of the beam width on the angular reflected energy when the substrate is gold. For a finite grating made of 15 slit of normalized period $D/\ell = 1.5$, illuminated by an obliquely incident Gaussian beam ($\theta_i = 30^\circ$) of wavelength λ/ℓ =0.9, and spot width $L/\ell = 7/\sqrt{2}, 10/\sqrt{2}, 50/\sqrt{2}, 5000/\sqrt{2}$.

sian beam ($\theta_i = 30°$) of width $L/\ell = 20/\sqrt{2}$, for the wavelengths λ/ℓ =0.1, 0.8, 1.5, and 2.5.

It is interesting compare these plots of Fig.13 with those given in transmission in Fig. 2, where the parameters are the same. From our calculations we get that the grating equation in reflection predict very well the position of the orders. We notice that the angular width of the orders is increased when the ratio between the wavelength and the width spot increase, *i.e.*, the angular width of the orders increase when λ/L also increase. This is true also in transmission as can be seen from Fig. 2.

4.3. Influence of the beam width

Now we consider the influence of the beam width on the angular reflected energy when the substrate is gold. In Fig. 14 are plotted the results for a finite grating made of 15 slit of normalized period $D/\ell = 1.5$, illuminated by an obliquely incident Gaussian beam ($\theta_i = 30°$) of wavelength λ/ℓ =0.9, and spot width $L/\ell = 7/\sqrt{2}$, $10/\sqrt{2}$, $50/\sqrt{2}$, $5000/\sqrt{2}$.

This Fig. 14 is the corresponding one of Fig. 6 in transmission, where the same parameters are taken into account. As we can see from these plots the property mentioned in Sec. 4.2 is also verified, *i.e.*, in transmission or in reflection the angular width of the orders increase when the ratio λ/L increase.

5. Conclusions

A rigorous modal theory for solving the diffraction of Gaussian beams by N equally spaced slits (finite grating) on a planar perfectly conducting screen was presented. We assume that the substrate is vacuum or conductor. The case of T.E. polarization and oblique incidence was considered. The study has been especially carried out in the vectorial region, where the polarization effects are important. The reflected and transmitted energy are analyzed as a function of several optogeometrical parameters: the wavelength, the beam width and the beam position, as well as the separation between slits (coupling).

Acknowledgments

The author J. Sumaya-Martinez acknowledge support from CONACYT-Mexico and UAEM under grants I35695-E and 1527/2001, respectively. The authors O. Mata-Mendez and F. Chavez-Rivas acknowledge support from Comision de Operaciones y Fomento de Actividades Academicas del Instituto Politecnico Nacional, Mexico.

1. E. Loewen and E. Popov, *Diffraction gratings and applications* (Marcel Dekker, Inc., New York 1997).
2. C.J. Bouwkamp, *Rep. Prog. Phys.* **17** (1954) 35.
3. C.C. Cheng, *IEEE Trans. Antennas Propag.* **AP-18** (1970) 660.
4. H.A. Kalhor, *J. Opt. Soc. Am.* **68** (1978) 1202.
5. G. Baldwin and A. Heins, *Math. Scand.* **2** (1954) 103.
6. Z.S. Agranovich , V.A. Marchenko, and V.P. Shestopalov, *Soviet Phys.-Tech. Phys.* **7** (1962) 277.
7. T. Otsuki, *J. Phys. Soc. Jpn.* **41** (1976) 2046.
8. K. Kobayashi and T. Inoue, *IEEE Trans. Antennas Propag.* **36** (1988) 1424.
9. R. Petit and G. Tayeb, *J. Opt. Soc. Am. A* **7** (1990) 1686.
10. T. Otsuki, *J. Opt. Soc. Am.* **7** (1990) 646.
11. L.A. DeAcetis and I. Lazar, *J. Opt. Soc. Am.* **62** (1972) 70.
12. L.A. DeAcetis and I. Lazar, *Appl. Opt.* **12** (1973) 2804.
13. L.A. DeAcetis, F.S. Einstein, R.A. Juliano, Jr., and I. Lazar, *Appl. Opt.* **15** (1976) 2866.
14. P. Kuttner, *Appl. Opt.* **15** (1976) 1199.
15. D. Marcuse, *Ligth Transmission Optics* (Van Nostrand Reinhold Co., New York 1982).
16. O. Mata-Mendez, *Opt. Lett.* **16** (1991) 1629.
17. O. Mata-Mendez and F. Chavez-Rivas, *Rev. Mex. Fis.* **39** (1993) 371.
18. O. Mata-Mendez, J. Sumaya-Martinez, and F. Chavez-Rivas, *Rev. Mex. Fís.* **41**(1995)807.
19. O. Mata-Mendez and F. Chavez-Rivas, *J. Opt. Soc. Am. A* **15** (1998) 2698.
20. O. Mata-Mendez and F. Chavez-Rivas, *J. Opt. Soc. Am. A* **18** (2001) 537
21. J. Sumaya-Martinez, O. Mata-Mendez, and F. Chavez-Rivas, *J. Opt. Soc. Am. A.* **20** (2003) 827.
22. O. Mata-Mendez and F. Chavez-Rivas, *Rev. Mex. Fís.* **39** (1993) 706.
23. M.A. Alvarez-Cabanillas and O. Mata-Mendez, *Rev. Mex. Fís.* **40** (1994) 846.
24. Palik D. Edward, *Handbook of optical constants of solid* (Academic Press Inc. 1985).